

# Caspase-mediated Cleavage Converts the Tumor Necrosis Factor (TNF) Receptor-associated Factor (TRAF)-1 from a Selective Modulator of TNF Receptor Signaling to a General Inhibitor of NF- $\kappa$ B Activation\*

Received for publication, October 30, 2002, and in revised form, March 17, 2003  
Published, JBC Papers in Press, April 22, 2003, DOI 10.1074/jbc.M211090200

Frank Henkler<sup>‡</sup>, Bernd Baumann<sup>§</sup>, Mariola Fotin-Mleczek<sup>‡</sup>, Monika Weingärtner<sup>‡</sup>,  
Ralph Schwenzer<sup>‡</sup>, Nathalie Peters<sup>‡</sup>, Angela Graness<sup>‡</sup>, Thomas Wirth<sup>§</sup>, Peter Scheurich<sup>‡</sup>,  
Johannes A. Schmid<sup>¶</sup>, and Harald Wajant<sup>‡</sup>||

From the <sup>‡</sup>Institute of Cell Biology and Immunology, University of Stuttgart, Allmandring 31, 70569 Stuttgart, Germany, the <sup>§</sup>Department of Physiological Chemistry, University of Ulm, Albert-Einstein-Allee 11, 89081 Ulm, Germany, and the <sup>¶</sup>Department of Vascular Biology and Thrombosis Research, University of Vienna, 1235 Vienna, Austria

**The role of tumor necrosis factor (TNF) receptor-associated factor (TRAF)-1 in NF- $\kappa$ B activation by various members of the TNF receptor family is not well understood, and conflicting data have been published. Here, we show that TRAF1 differentially affects TRAF2 recruitment and activation of NF- $\kappa$ B by members of the TNF receptor family. Interestingly, a naturally occurring caspase-derived cleavage product of TRAF1 solely comprising its TRAF domain (TRAF1-(164–416)) acted as a general inhibitor of NF- $\kappa$ B activation. In contrast, a corresponding fragment generated by cleavage of TRAF3 showed no effect in this regard. In accordance with these functional data, TRAF1, but not TRAF3, interacted with the IKK complex via its N-TRAF domain. Endogenous TRAF1 and the overexpressed TRAF domain of TRAF1 were found to be constitutively associated with the IKK complex, whereas endogenous receptor interacting protein was only transiently associated with the IKK complex upon TNF stimulation. Importantly, the caspase-generated TRAF1-fragment, but not TRAF1 itself inhibited IKK activation. Our results suggest that TRAF1 and TRAF1-(164–416) exert their regulatory effects on receptor-induced NF- $\kappa$ B activation not only by modulation of TRAF2 receptor interaction but especially TRAF1-(164–416) also by directly targeting the IKK complex.**

characterized by a carboxyl-terminal homology domain of about 180 amino acids, named the TRAF domain. Apart from TRAF1, all TRAF proteins show a similar overall architecture in their amino-terminal part: a single RING finger, which is followed by five or seven evenly separated zinc finger motifs (1–3). TRAF proteins have been recognized as mediators of NF- $\kappa$ B activation and regulators of cell death, but also as activators of various kinases including ERK, JNK, and IRE1 $\alpha$  (1–3). The TRAF proteins can interact with a plethora of proteins that play a role in the signaling pathways mentioned above via their TRAF domain. However, in a minority of cases associations can also occur via the amino-terminal ring/zinc finger domain. The carboxyl-terminal part of the TRAF domain allows direct binding to various TNF receptors (1–3). Thus, the TRAF molecules seem to act mainly as adaptor and scaffolding proteins. Several lines of evidence, especially analyses of knock-out mice, point to a critical role of TRAF2, TRAF5, and TRAF6 in TNF receptor and IL1R/Toll receptor-induced activation of JNK and the kinases of the IKK complex (1–3). Although the molecular mode of TRAF4 action is poorly understood, analyses of knock-out mice (4, 5) and the TRAF4 expression pattern (6, 7) argue for a role of this molecule in epithelial-mesenchymal interactions and neurogenesis. The functions of TRAF1 and TRAF3 are rather unknown.

With respect to its molecular architecture, TRAF1 is a unique member of the TRAF family. TRAF1 has a carboxyl-terminal TRAF domain as the other members of the TRAF family; however, the amino-terminal part of TRAF1 contains only a single zinc finger and shows no homologies to other proteins (8, 9). TRAF1 is able to interact with TRAF2 and the caspase inhibitory proteins cIAP1 and cIAP2 (8, 10). These proteins act cooperatively to suppress activation of caspase-8 and TNF-induced apoptosis (11). In accordance with an anti-apoptotic function of TRAF1, transgenic mice that overexpress this molecule showed reduced antigen-induced apoptosis of CD8(+) T-lymphocytes (12). Besides its anti-apoptotic function, TRAF1 seems to have also anti-proliferative effects as TRAF1(–/–) T-cells exerted stronger proliferation than wild-type T-cells after T-cell receptor or TNF-R2 stimulation (13). Although TRAF1 itself does not activate NF- $\kappa$ B upon transient overexpression, it is involved in the regulation of this pathway, possibly due to its interaction with TRAF2. However, the role of TRAF1 in regulation of NF- $\kappa$ B seems to be complex, as some studies found an inhibitory effect of TRAF1 on NF- $\kappa$ B activation whereas others did not (13–17). Remarkably, TRAF1 is transcriptionally up-regulated by NF- $\kappa$ B and could have a role

The tumor necrosis factor (TNF)<sup>1</sup> receptor-associated factor (TRAF) family of proteins has a pivotal role in signaling by members of the TNF receptor and the interleukin-1 receptor/Toll-like receptor (IL1R/TLR) family (1–3). TRAF proteins are

\* This work was supported by Deutsche Forschungsgemeinschaft Grants Wa 1025/3-1, SFB 495/A5, and SFB 497/B1. The costs of publication of this article were defrayed in part by the payment of page charges. This article must therefore be hereby marked "advertisement" in accordance with 18 U.S.C. Section 1734 solely to indicate this fact.

|| To whom correspondence should be addressed: Dept. of Molecular Internal Medicine, Medical Polyclinic, University of Wuerzburg, Roentgenring 11, 97070 Wuerzburg, Germany. Tel.: 49-931-201-71000; Fax: 49-931-201-71070; E-mail: harald.wajant@mail.uni-wuerzburg.de.

<sup>1</sup> The abbreviations used are: TNF, tumor necrosis factor; FADD, Fas-associating protein with death domain; GFP, green fluorescent protein; IKK, inhibitor of  $\kappa$ B (I- $\kappa$ B) kinase; TRAF, TNF receptor-associated factor; TRADD, TNFR1-associated death domain protein; FLIP, fluorescence loss in photobleaching; FRAP, fluorescence recovery after photobleaching; HEK, human embryonic kidney; CHX, cycloheximide; ROI, regions of interest; FIT, filament interaction trap; FACS, fluorescence-activated cell sorting; mAb, monoclonal antibody.

in receptor cross-talk and/or feedback regulation of activated receptor signaling complexes. Moreover, TRAF1 can be cleaved during apoptosis by caspase-8 (18, 19). The carboxyl-terminal cleavage product of TRAF1 produced thereby comprises only the TRAF domain of the molecule, is still able to interact with TRAF2 and interferes with TNF-induced NF- $\kappa$ B activation (18, 19).

Here, we show that TRAF1 and its cleavage product selectively interfere with the recruitment of TRAF2 to some members of the TNF receptor family and demonstrate that the caspase-derived carboxyl-terminal fragment of TRAF1, but not full-length TRAF1, blocks NF- $\kappa$ B activation at the level of the IKK complex. Together, these data reveal that caspase-mediated cleavage converts TRAF1 from a selective modulator of TNF receptor signaling to a general inhibitor of NF- $\kappa$ B activation suggesting that the IKK complex is the target of the NF- $\kappa$ B-inhibitory TRAF1-fragment.

#### EXPERIMENTAL PROCEDURES

**Reagents, Cell Lines, and Antibodies**—The expression constructs for TRADD, NIK, TRAF2, p50, and p65 were kind gifts from D. Goeddel (Tularik Inc., South San Francisco, CA), D. Wallach (Weizmann Institute of Science), H. Engelmann (University of Munich), A. Israel (Institut Pasteur), and R. M. Schmid (University of Ulm, Germany). HeLa cells and the human T-cell line DII/23-7 were maintained in RPMI 1640 medium containing 5% (HeLa) and 10% (DII/23-7) heat-inactivated fetal calf serum. Jurkat T-cells and SV80 cells were grown in Dulbecco's modified Eagle's medium (Invitrogen) supplemented with 10% fetal calf serum. Medium for Jurkat T-cells was in addition supplemented with 50  $\mu$ M  $\beta$ -mercaptoethanol. IKK $\alpha$ -GFP and IKK $\beta$ -GFP expression constructs have already described elsewhere (20). To generate expression constructs encoding TRAF1-GFP, TRAF1-NT-GFP, TRAF1-NTD-GFP, and TRAF1-CTD-GFP, cDNA fragments corresponding to amino acids 1–416 (TRAF1), 1–193 (TRAF1-NT), 184–270 (TRAF1-NTD including a start ATG), and 263–416 (TRAF1-CTD) of TRAF1 were amplified by PCR and cloned into the *Bgl*II and *Sac*II sites of pEGFP-N1 (TRAF1, TRAF1-NT, TRAF1-NTD) and pEGFP-C1 (TRAF1-CTD). For this purpose the primers used for PCR amplification contained *Bgl*II or *Bam*H1 (compatible with *Bgl*II) and *Sac*II restriction sites in their 5' overhang. TRAF1-TD-GFP was obtained by replacing the death domain of FADD in the pcDNA3-GFP- $\Delta$ FADD construct described elsewhere (21) by a TRAF1 cDNA fragment encompassing amino acids 186–416 using *Bam*H1 and *Not*I. To allow deletion of the FADD part from pcDNA3-GFP- $\Delta$ FADD via *Bam*H1 and *Not*I, a *Bam*H1/*Bgl*II hybrid site between the amino-terminal GFP and the carboxyl-terminal FADD part has before restored to a *Bam*H1 site and a *Bam*H1 site present 5' to the start codon of the fusion protein has been deleted. The IKK $\gamma$ -GFP encoding expression plasmid was obtained by cloning a PCR fragment containing amino acids 1–419 of IKK $\gamma$  into the *Bgl*II and *Sac*II restriction sites of pEGFP-N1. The expression vector encoding IKK $\gamma$ -TRADD (169–312) was obtained from the pEGFP-N1-IKK $\gamma$  plasmid by replacing the GFP part with a PCR fragment corresponding to amino acids 169–312 of TRADD using the *Sac*II and *Not*I site of pEGFP-N1. EGFP FACS calibration beads were purchased from BD Biosciences Clontech (Heidelberg, Germany).

**Induction and Detection of TRAF2 Receptor Complexes**—HeLa cells which stably express either CD40, CD30, TNF-R2, or a TNF-R2-LT $\beta$  fusion receptor were grown on square slides (18  $\times$  18 mm) and transfected with 1.5  $\mu$ g of a TRAF2-GFP encoding plasmid, using SuperFect reagent (Qiagen). After 18 h, HeLa-CD40 cells were stimulated with 300 ng/ml FLAG-tagged CD40L, which was secondarily cross-linked with 1  $\mu$ g/ml of the FLAG-specific mAb M2. HeLa-CD30 cells were left untreated, since auto-aggregation of CD30 occurred in these cells without requirement of further stimulation. HeLa-TNF-R2 cells and HeLa-TNF-R2-LT $\beta$  cells were treated with an agonistic TNF-R2 IgG fraction (2  $\mu$ g/ml). After one hour cells were fixed, using methanol/acetone (1:1, v/v). Receptor-TRAF2-GFP complexes were visualized by immunofluorescence staining, as described below and analyzed using a Leica IMRE microscope. Slides, which were only examined for expression and localization of GFP fusion proteins were fixed in 3% paraformaldehyde and examined by fluorescence microscopy.

**Luciferase Assay**—HEK293 cells (20,000 cells per well of a 96-well plate) were transiently cotransfected with 0.07 ng of a NF- $\kappa$ B luciferase reporter construct, 0.03 ng of a  $\beta$ -galactosidase expression vector and 60 ng of a mixture of the indicated expression constructs, or empty vector

with SuperFect (Qiagen, Hilden, Germany) according to the manufacturer's recommendations. After 24 h, cells were harvested in phosphate-buffered saline, lysed in luciferase lysis buffer (Promega, Mannheim, Germany), and assayed for luciferase and  $\beta$ -galactosidase activities using an LUMAT 9501 Luminometer (Berthold, Bad Wildbad, Germany). Transfections were done in triplicates. The absolute values of NF- $\kappa$ B activation were normalized in respect to the  $\beta$ -galactosidase activities, in order to control variations in transfection efficiencies.

**Coimmunoprecipitation of IKK Complex-associated Proteins and Immunoblotting**—For endogenous coimmunoprecipitation experiments, cells ( $200 \times 10^6$ ) were treated with the reagents of interest for the indicated times. Then 4 volumes of ice-cold phosphate-buffered saline were added to arrest the signaling status of the cells. All the following procedures were performed on ice or at 4  $^{\circ}$ C. Cells were washed one time with phosphate-buffered saline, centrifuged, and resuspended in 50 mM Tris, 400 mM NaCl/10% glycerol, pH 7.4 (1 ml per  $100 \times 10^6$  cells). For cell lysis 0.1 volumes of a protease inhibitor mixture (Roche Applied Science) and Nonidet P-40 to a final concentration of 0.1% were added. After 45 min on ice the lysates were centrifuged at 15,000 rpm for 20 min. The supernatant was divided in two groups, which were incubated under gentle agitation with either 5  $\mu$ g of anti-IKK $\alpha$  mAb B78-1 (BD Pharmingen, Hamburg, Germany) or the respective control antibody (mouse IgG<sub>2b</sub>, Dianova, Hamburg, Germany) for 2 h. Then 60  $\mu$ l of a 1:1 slurry of protein G-Sepharose Fast Flow (Amersham Biosciences) were added for another hour of incubation. The Sepharose beads were washed four times with low salt buffer (1% Triton, 20 mM Tris, 150 mM NaCl, 1 mM EDTA, pH 7.5) supplemented with 0.1 volumes of a protease inhibitor mixture (Roche Applied Science), separated on a 12.5% SDS-PAGE and transferred to a nitrocellulose membrane. Immunoblotting analysis were performed with the anti-TRAF1 rabbit polyclonal antibody H-125 (Santa Cruz Biotechnology, Heidelberg, Germany), the anti-RIP mAb G322-2 (BD Pharmingen) and the anti-IKK $\alpha$  mAb already used for immunoprecipitation. Visualization was done with horseradish peroxidase-coupled goat anti-rabbit-IgG, horseradish peroxidase-coupled goat anti-mouse-IgG and NBT and BCIP as substrate.

**IKK Kinase Assay**—HEK293 or Jurkat cells were transfected by electroporation with a VSV epitope-tagged IKK $\beta$  expression plasmid along with the indicated plasmids. 16–24 h after transfection cells were lysed Nonidet P-40 lysis buffer containing 50 mM Tris, pH 7.6, 137 mM NaCl, 1% Triton X-100, 1 mM EDTA, 1 mM EGTA, 1 mM Na<sub>3</sub>VO<sub>4</sub>, 10 mM  $\beta$ -glycerophosphate, 1 mM dithiothreitol supplemented with a protease inhibitor mixture (Roche Applied Science). VSV-IKK $\beta$  containing complexes were immunoprecipitated from 1 mg extract using a VSV specific antibody (clone P5D4; Sigma). The precipitated complex was incubated in kinase assay mixture containing 25 mM HEPES (pH 7.5), 150 mM NaCl, 25 mM  $\beta$ -glycerophosphate, 10 mM MgCl<sub>2</sub>, 1 mM dithiothreitol, 10  $\mu$ Ci [ $\gamma$ -<sup>32</sup>ATP], and 600 ng of GST-I $\kappa$ B $\alpha$  substrate. After 20 min (30  $^{\circ}$ C) the reaction was terminated by boiling with SDS sample buffer, and the proteins were separated on 10% polyacrylamide gels. Finally, the proteins were electrotransferred to a polyvinylidene difluoride membrane, and radioactive bands were visualized by PhosphorImager or autoradiography. The membranes were used for immunoblot analysis with antibodies specific for IKK $\beta$  (Santa Cruz Biotechnology, sc-7606).

**Immunofluorescence and Confocal Microscopy**—Cells fixed onto coverglasses were blocked for 20 min with phosphate-buffered saline, 3% bovine serum albumin. HeLa-CD30 cells were treated for 1 h with a CD30-specific monoclonal antibody (0.25  $\mu$ g/ml). As antibody reagents were used to induce receptor complex formation in the other cell lines, no primary antibodies were applied. Slides were then incubated for 45 min with Alexis 546-conjugated anti-mouse or anti-rabbit sera (1:250 diluted) and analyzed by confocal fluorescence microscopy.

**Determination of Dissociation and Association Kinetics of TRAF1-GFP and TRAF1-TD-GFP**— $5 \times 10^5$  HeLa cells were electroporated with 3.5  $\mu$ g of IKK $\gamma$ -DD, and 6.5  $\mu$ g of either TRAF1-GFP or TRAF1-TD-GFP expression plasmids and seeded into MATEK cell culture dishes that contained cover glass inlets. Confocal on-line microscopy was performed on an inverted Leica DM microscope. Cells were maintained at 37  $^{\circ}$ C and 5% CO<sub>2</sub> during analysis in a preconditioned chamber. Dissociation kinetics were determined by fluorescence loss in photobleaching (FLIP). Regions of interest (ROIs) were defined that excluded IKK $\gamma$ -DD filaments associated with TRAF1-GFP or TRAF1-TD-GFP, but covered most of the remaining cell area. The ROI of selected cells were bleached for 6 min with high laser intensity and subsequently ROIs were bleached for 1 min, followed by imaging of the entire cell in up to 20 cycles using the time-lapse function of the Leica confocal microscope software. Relative fluorescence intensities in the indicated regions were quantified, using the Leica confocal software.

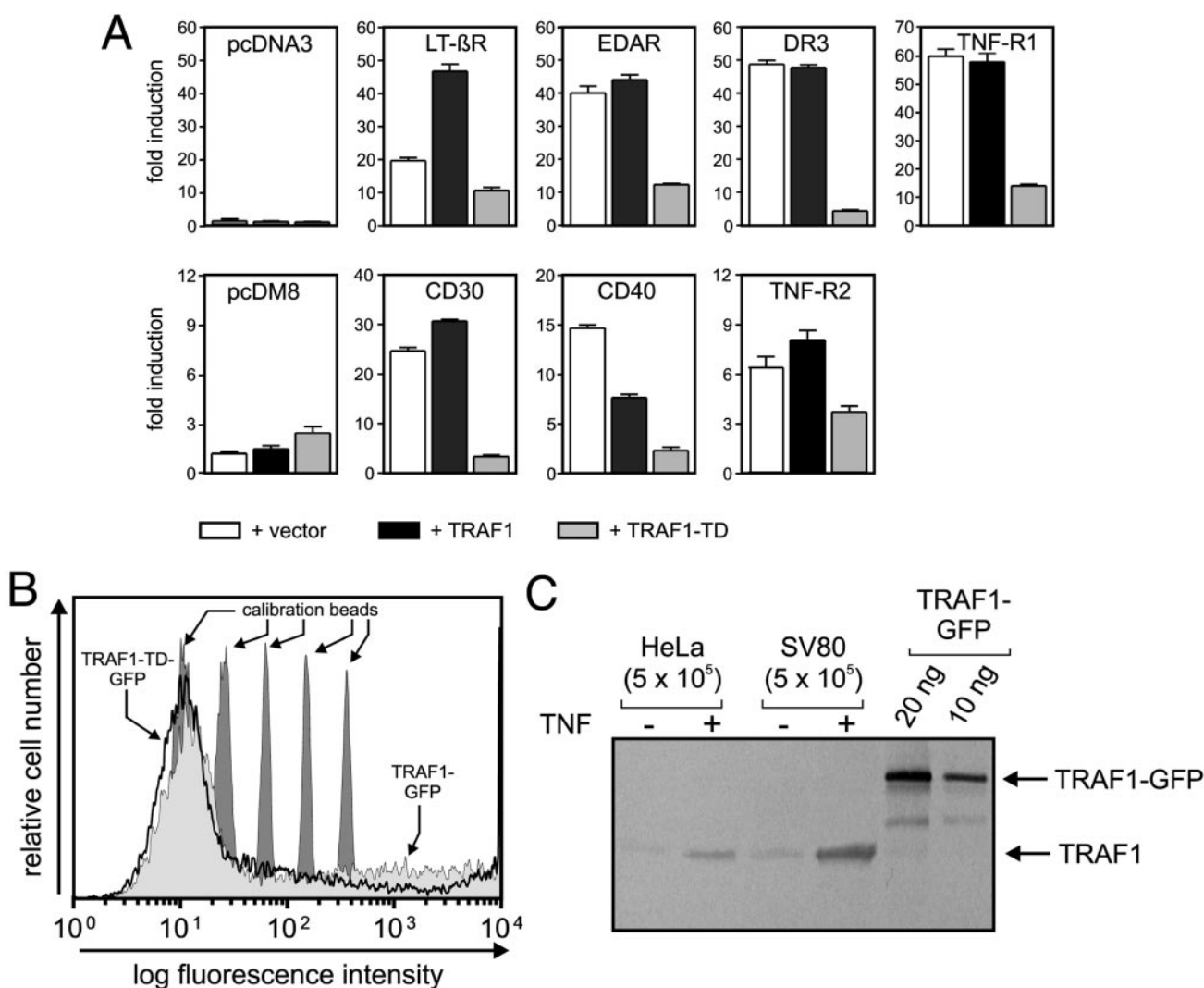


**FIG. 1. The caspase-derived TRAF domain fragment of TRAF1 acts as a general inhibitor of receptor-mediated NF- $\kappa$ B activation.** *A*, HEK293 cells were cultured in 96-well plates and transfected with 0.07  $\mu$ g of NF- $\kappa$ B and 0.03  $\mu$ g of  $\beta$ -galactosidase reporter plasmid, per well. Cells were co-transfected with 0.03  $\mu$ g of expression constructs encoding the indicated receptors and a 4-fold excess (0.12  $\mu$ g) of either empty vector (white boxes), TRAF1 (black boxes), or TRAF1-TD (gray boxes) expression plasmids. pcDNA3 served as empty vector control for the LT $\beta$ R, EDAR, DR3 and TNF-R1 expression plasmids, pcDM8 for CD30, CD40, and TNF-R2 expression plasmids. Experiments were done in triplicates. Luciferase and  $\beta$ -galactosidase were measured as described under "Experimental Procedures." Relative activations of NF- $\kappa$ B are indicated. *B*, FACS analysis of EGFP FACS Calibration beads loaded with 0, 4,500, 15,000, 44,000, and 116,000 molecules of equivalent soluble fluorochrome and HEK293 cells expressing TRAF1-GFP and TRAF1-TD-GFP, 24 h post-transfection. *C*, quantification of endogenous TRAF1 expression.  $5 \times 10^5$  HeLa or SV80 cells were stimulated with TNF (20 ng/ml) for 6 h or remained untreated. Lysates were prepared and analyzed by Western blotting with a GFP-TRAF1 mass standard and a TRAF1-specific polyclonal antibody.

Association kinetics were determined by fluorescence recovery after photobleaching (FRAP). In these experiments, ROIs were defined around filaments and bleached for 4 min. Recovery of fluorescence in the bleached areas was analyzed over 15 min whereby cells were imaged every 1 min.

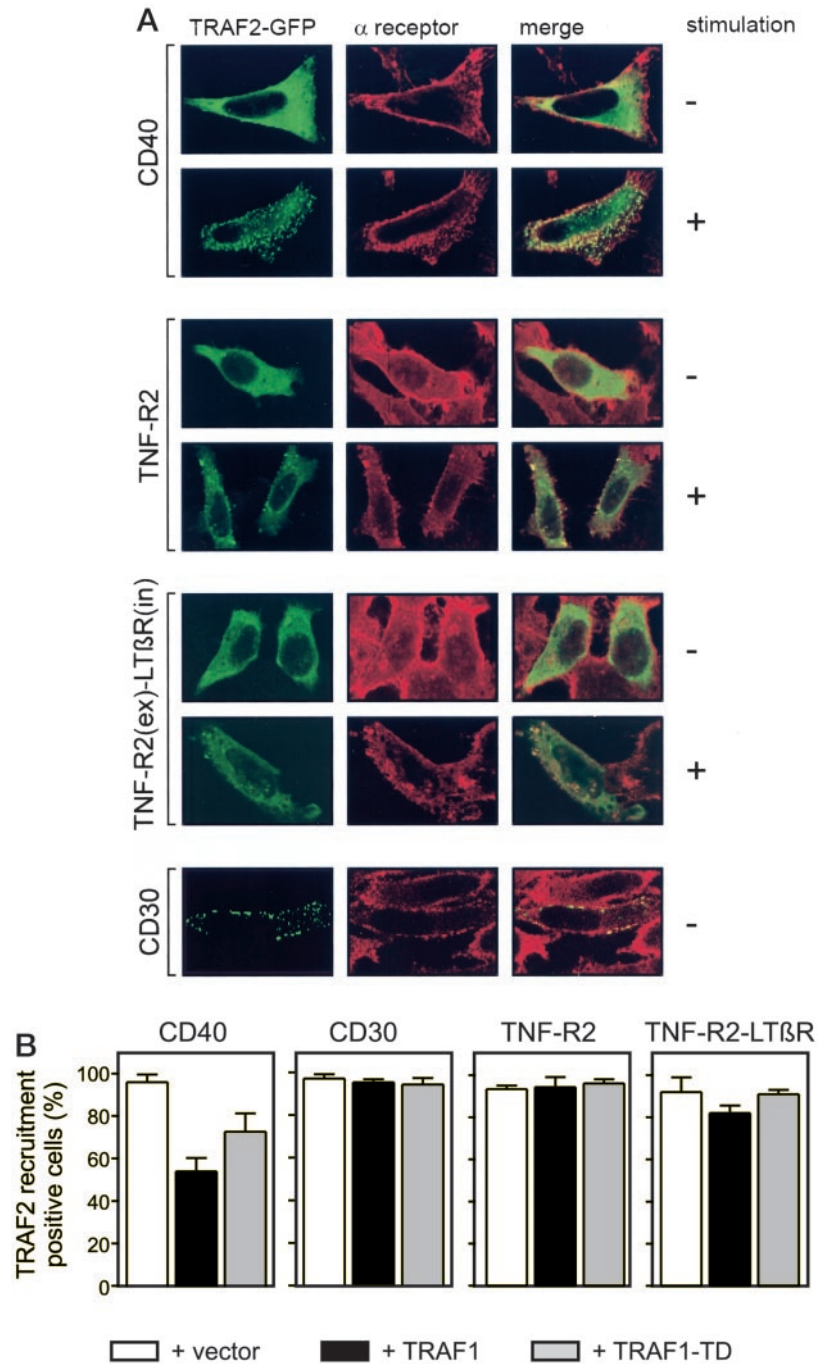
**Yeast Two-hybrid Analysis**—Bait vectors for IKK $\alpha$  (amino acids 272–745), IKK $\beta$  (amino acids 466–756) and full-length IKK $\gamma$  were derived by cloning the corresponding cDNAs in-frame to the Gal4 binding domains of pGBKT7, pAS2–1, and pBRIDGE (BD Clontech, Heidelberg, Germany), respectively. Vectors encoding human TRAF1 and TRAF3 cDNA fused to the Gal4 activation domain were kindly provided by David Sassoon (Mount Sinai School of Medicine, New York). Two-hybrid analysis were performed in the yeast strain Y187 (BD Clontech). Finally, colonies were assayed for  $\beta$ -galactosidase activity.

## RESULTS

**TRAF1 and Its Caspase-derived Carboxyl-terminal Fragment Differentially Affect NF- $\kappa$ B Activation**—Inhibitory, but also stimulatory or neutral effects of TRAF1 on receptor-induced NF- $\kappa$ B activation have been reported (13–17). Thus, the

effects of TRAF1 on NF- $\kappa$ B activation are rather unclear. We have addressed this question by analyzing the impact of TRAF1 on a range of NF- $\kappa$ B-inducing receptors of the TNF receptor family in transient reporter gene assays. As a caspase-generated, truncated form of TRAF1 occurs naturally during apoptosis (18, 19), we included an expression plasmid encoding this fragment (TRAF1 amino acids 164–416, designated as TRAF1-TD) in our analysis. With exception of a significant inhibitory effect of full-length TRAF1 on CD40-mediated NF- $\kappa$ B activation, we found no evidence for a major inhibitory effect of transient TRAF1 expression on the following NF- $\kappa$ B stimulators: CD30, TNF-R2, LT $\beta$ R, EDAR, DR3, and TNF-R1 (Fig. 1A). In contrast, overexpression of TRAF1-TD inhibited all of these NF- $\kappa$ B inducers (Fig. 1A). Although it has already been shown elsewhere that the caspase-generated cleavage product of TRAF1 inhibits TNF-mediated NF- $\kappa$ B activation (18, 19), our data show further that this TRAF domain com-

**FIG. 2. Effects of TRAF1 and TRAF1-TD on TRAF2 recruitment by activated members of the TNF receptor family.** *A*, HeLa cells stably expressing CD40, TNF-R2, CD30, or a TNF-R2-LT $\beta$ R fusion protein were grown on glass slides and were transiently co-transfected with TRAF2-GFP (20% of total DNA) and either empty vector, TRAF1-, or TRAF1-TD expression vectors (80% of total DNA). Receptors were stimulated for 1 h (except in HeLa-CD30 cells), as described under "Experimental Procedures." Cells were fixed (methanol/acetone 1:1, v/v), and receptors were visualized in stimulated (+) and non-stimulated (-) cells by immunofluorescence staining. Slides were analyzed for receptor-TRAF2-GFP co-localization by confocal fluorescence microscopy. Please note that in HeLa-CD30 cells, auto-aggregation of the receptor occurred without requirement of stimulation. *B*, receptor-induced TRAF2-GFP clustering was analyzed in cells, co-transfected with a TRAF2-GFP expression plasmid and a 4-fold excess of either empty vector (*white boxes*), or expression constructs encoding TRAF1 (*black boxes*) and TRAF1-TD (*gray boxes*). Forty randomly selected cells were analyzed for recruitment of TRAF2-GFP into receptor clusters. Recruitment assays were carried out as triplicates.



prising fragment of TRAF1 can act as a general inhibitor of NF- $\kappa$ B activation. Reporter gene analysis with GFP fusion proteins of TRAF1 and TRAF1-TD showed the same results (data not shown). FACS analysis of these GFP fusion proteins and EGFP FACS calibration beads revealed that around 50% of successfully transfected cells expressed more than 116,000 molecules of GFP fusion proteins per cell, whereas the rest of the cells expressed between 4000 and 116,000 molecules per cell (Fig. 1B). Endogenous TRAF1 expression of up to 20 fg per cell corresponding to 300,000 molecules per cell was observed upon TRAF1 up-regulation by NF- $\kappa$ B inducers such as TNF (Fig. 1C). As the inhibitory effects on NF- $\kappa$ B activation described above are between 50 and 90%, these data indicate that "physiological" levels of TRAF1-TD and TRAF1 may be sufficient to mediate the effects described above.

*TRAF1 and Its Caspase-derived Carboxyl-terminal Fragment Inhibit Selectively TRAF2 Recruitment to Sites of CD40 Signaling*—We have recently found that the inhibitory effect of TRAF1 on CD40-induced NF- $\kappa$ B activation correlates with an inhibitory effect of TRAF1 on TRAF2 recruitment to sites of CD40 signaling complex formation.<sup>2</sup> Although TRAF2 is known to recruit TRAF1 into the CD40 signaling complex, TRAF1 expression also led to an overall reduction of TRAF2 recruitment to ligand-induced CD40 clusters.<sup>2</sup> As TRAF1 has also been suggested to be a part of the receptor signaling complexes of CD30 (22, 23) and TNF-R2 (8), we analyzed the effect of increasing expression of TRAF1 or TRAF1-(164–416) on

<sup>2</sup> H. Wajant, F. Henkler, and M. Fotin-Mleczek, manuscript submitted.

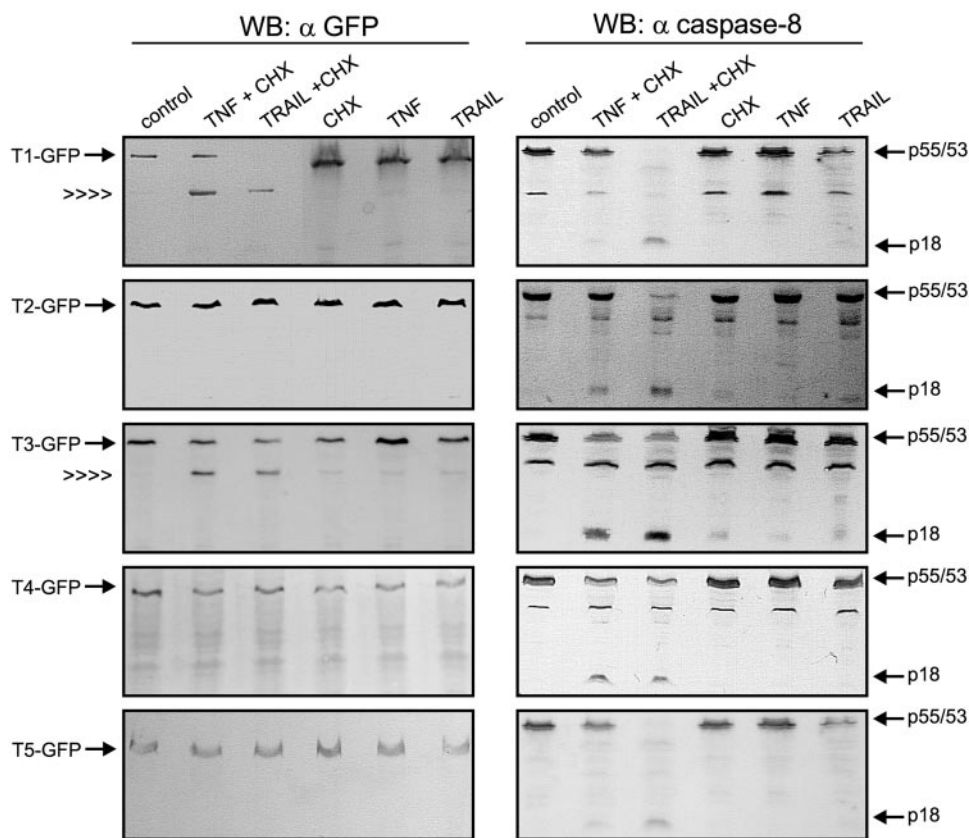
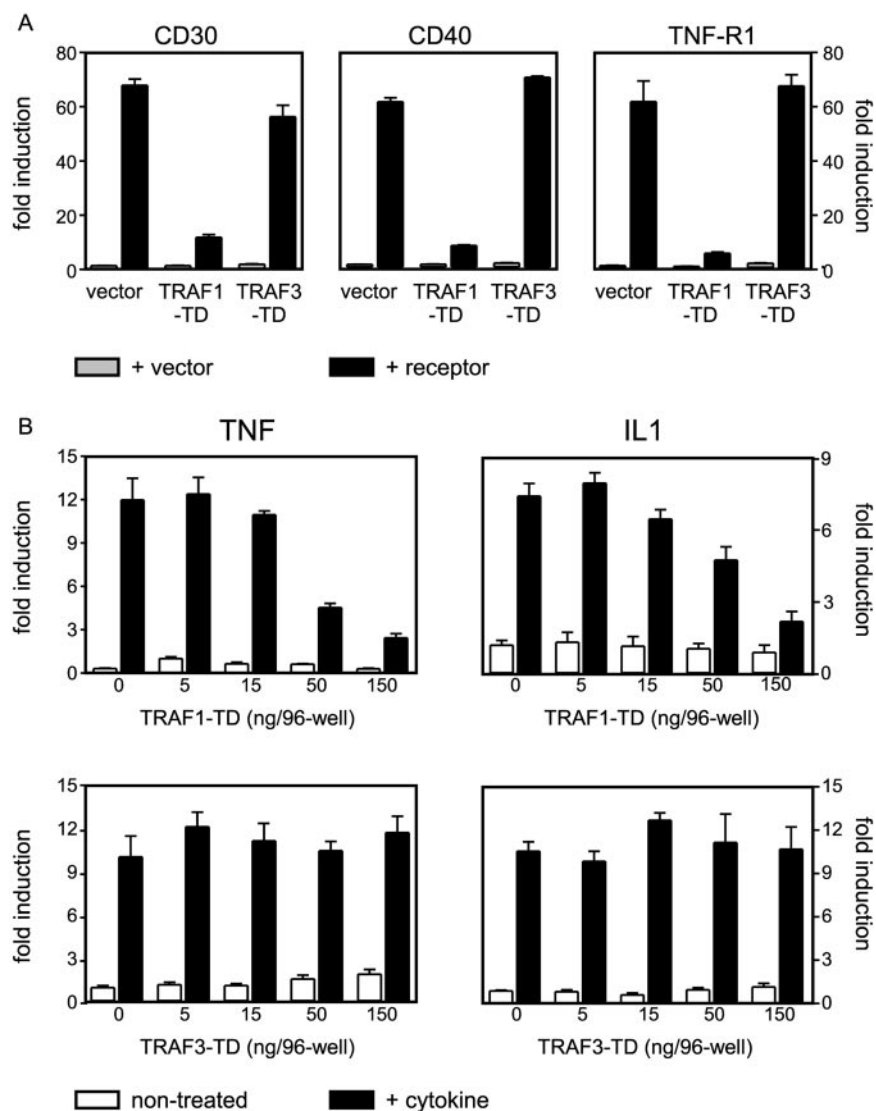


**FIG. 3. Generation of TRAF1 and TRAF3 cleavage products correlates with induction of apoptosis and activation of caspase-8.** HeLa cells stably expressing the TRAF-GFP fusion proteins indicated on the *left side* (*T1-GFP*, TRAF1-GFP; *T2-GFP*, TRAF2-GFP; *T3-GFP*, TRAF3-GFP; *T4-GFP*, TRAF4-GFP; *T5-GFP*, TRAF5-GFP) were treated for 10 h with the indicated combinations of TNF (100 ng/ml), FLAG-tagged TRAIL (100 ng/ml) cross-linked with the FLAG-specific mAb M2 (1  $\mu$ g/ml) and 2.5  $\mu$ g/ml CHX. Co-treatment with CHX is necessary to reduce expression of anti-apoptotic factors and facilitates apoptosis induction by TNF and TRAIL. Cell lysates were analyzed by Western blotting, using a GFP-specific mAb to detect the TRAF fusion proteins (*left panel*). Caspase-derived cleavage products containing the carboxyl-terminal parts of TRAF1 or TRAF3 fused to the GFP tag are indicated by *arrowheads*. In parallel, corresponding blots were analyzed, using a caspase-8-specific monoclonal antibody (*right panel*). Activation of caspase-8 is indicated by degradation of the pro-caspase precursor (p55/53) and appearance of an 18 kDa cleavage product (marked on the *right side*).

TRAF2 recruitment to these receptors. In addition, we analyzed TRAF2 recruitment to the lymphotoxin- $\beta$  receptor (LT $\beta$ R), a member of the TNF receptor family that is believed to signal independently of TRAF1. For this purpose, we determined the recruitment efficiencies of a TRAF2-GFP fusion protein to CD40, CD30, TNF-R2, and to a chimeric receptor consisting of the extracellular domain of TNF-R2 and the cytoplasmic domain of LT $\beta$ R (TNF-R2ex-LT $\beta$ Rin), using fluorescence microscopy. Stimulation of CD40, TNF-R2, or TNF-R2ex-LT $\beta$ Rin in HeLa cells stably expressing these receptors led to receptor clustering (Ref. 24 and data not shown), whereas in HeLa-CD30 cells auto-aggregation of the receptor was observed already without stimulation. Confocal laser microscopy showed that TRAF2-GFP was recruited into small aggregates co-localizing with the induced receptor clusters in consequence of receptor stimulation (Fig. 2A). As no co-localization of TRAF2-GFP with CD40, TNF-R2, or with the TNFR2ex-LT $\beta$ Rin fusion receptor was apparent without stimulation, we used the ligand-induced clustering of TRAF2 and receptors as an early indication of activated receptor signaling and analyzed further, whether TRAF1 expression can interfere with this process. Receptor stimulation led to formation of multiple TRAF2-GFP receptor clusters in the vast majority of cells. To quantify a potential inhibitory effect of TRAF1 on TRAF2-GFP receptor clustering, we determined the proportion of cells with no or less than 5 TRAF2-GFP aggregates per activated cell. Consistent with our earlier observations, we found that the portion of cells, where CD40L-induced TRAF2-GFP aggregate formation oc-

curred, was almost 100% in this assay, when TRAF2-GFP was cotransfected with empty vector. This portion decreased to about 50% when the TRAF2-GFP expression plasmid was cotransfected with a 4-fold excess of TRAF1 expression plasmid (Fig. 2B). In contrast, an excess of TRAF1 showed no effect on the formation of TRAF2-GFP aggregates, neither in TNF-R2ex-LT $\beta$ Rin- and TNF-R2-expressing cells stimulated with an agonistic TNF-R2-specific IgG fraction, nor on the capacity of TRAF2-GFP to co-localize with CD30 clusters resulting from auto-aggregation of this receptor in HeLa-CD30 cells (Fig. 2B). Expression of TRAF1-TD modulated the interactions between activated, clustered receptors and TRAF2-GFP in a similar way as TRAF1 (Fig. 2B). The selective inhibitory effect of TRAF1 on CD40-induced NF- $\kappa$ B activation correlated with the ability of TRAF1 to interfere with the recruitment of TRAF2 to CD40 clusters without affecting TRAF2 recruitment by other receptors. Thus, TRAF1 blocks CD40-mediated NF- $\kappa$ B activation by inhibition of TRAF2 recruitment. However, the general NF- $\kappa$ B inhibitory effect of the caspase-derived carboxyl-terminal TRAF1 cleavage product cannot be related to interference with TRAF2 receptor interactions. Thus, the receptor-selective inhibitory effect of TRAF1 and the global NF- $\kappa$ B inhibitory effect of the caspase-generated TRAF1-(164–416) fragment must be based on different mechanisms.

*The Caspase-derived Carboxyl-terminal Fragment of TRAF3 Has No NF- $\kappa$ B Inhibitory Capability*—While TRAF2, TRAF4, TRAF5, and TRAF6 are not cleaved during apoptosis, TRAF3 has recently been identified as a caspase substrate (Ref. 25 and



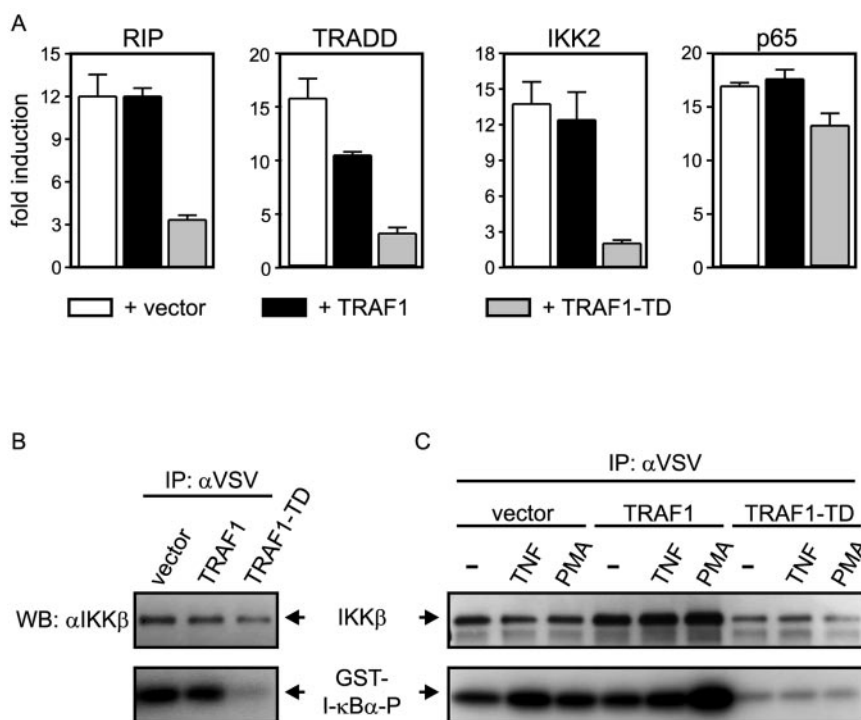
**FIG. 4. TRAF1-TD, but not TRAF3-TD, inhibits activation of NF- $\kappa$ B.** *A*, HEK293 cells were cultured in 96-well plates and transfected with 0.07  $\mu$ g of NF- $\kappa$ B and 0.03  $\mu$ g of  $\beta$ -galactosidase reporter plasmid along with 0.03  $\mu$ g of the indicated receptor expression vectors (black boxes) or empty vector (gray boxes) as a control and a 4-fold excess of empty vector, or expression vectors encoding TRAF1-TD or TRAF3-TD. Expression of reporter genes was measured, as described under "Experimental Procedures." *B*, HEK293 cells were transfected with NF- $\kappa$ B and  $\beta$ -galactosidase reporter constructs, as described above along with the indicated amounts of either TRAF1-TD or TRAF3-TD expression vectors. The total amount of DNA was adjusted to 250 ng per well, using pcDNA3. Next day, cells were stimulated with 25 ng/ml TNF (black bars, left column) or 10 ng/ml IL1 (black bars, right column) for 7 h or left untreated (open bars). Finally, relative activation of NF- $\kappa$ B was determined.

Fig. 3). As in the case of TRAF1, caspase-mediated cleavage of TRAF3 led to the release of a truncated TRAF molecule, which contains the TRAF domain, but not the amino-terminal zinc fingers or the RING finger motif (25). To verify whether this caspase-derived cleavage product possesses a NF- $\kappa$ B inhibitory potential similar to the corresponding TRAF1 fragment, we analyzed an analogous deletion mutant of TRAF3 (TRAF3-TD). As already shown in Fig. 1 TRAF1-TD blocked NF- $\kappa$ B activation by overexpressed CD40, CD30, and TNF-R1 as well as upon stimulation with TNF and IL1. In contrast to TRAF1-TD, the corresponding TRAF3 fragment (TRAF3-TD) never showed a NF- $\kappa$ B-inhibitory effect (Fig. 4), suggesting that the caspase-derived cleavage products of TRAF1 and TRAF3 have non-redundant functions during apoptosis.

**The TRAF Domain of TRAF1 Inhibits NF- $\kappa$ B Activation at the Level of the IKK Complex**—To analyze which step of the NF- $\kappa$ B signaling pathway is the target of TRAF1-TD, we co-transfected a NF- $\kappa$ B-dependent reporter construct together with expression constructs encoding TRAF1-(164–416) and various known compounds of this signaling pathway into 293 cells. As shown in Fig. 5A, TRADD, RIP, IKK $\beta$ , and p65 were each able to robustly stimulate the NF- $\kappa$ B-dependent reporter gene. When the same expression constructs were co-transfected with the TRAF1-TD expression vector, we found a strong inhibitory effect on all of these NF- $\kappa$ B-inducers, except p65, which was only modestly affected (Fig. 5A). This suggests that

the TRAF1-derived TRAF domain exerts its NF- $\kappa$ B-inhibitory effect by interference with a component of this signaling pathway, which acts either at the level of the IKK complex or immediately downstream of it. To further verify a possible effect of TRAF1 or TRAF1-TD on the IKK complex we performed immunocomplex kinase assays. For this purpose VSV-tagged IKK $\beta$  was cotransfected into HEK293 (Fig. 5B) and Jurkat T-cells (Fig. 5C) with either empty vector or expression constructs encoding TRAF1 and TRAF1-TD. The epitope-tagged IKK $\beta$  protein was immunoprecipitated with an anti VSV antibody and assayed for kinase activity with a GST-fusion protein containing the amino-terminal domain of I- $\kappa$ B $\alpha$  in the presence of [ $\gamma$ - $P^{32}$ ]ATP. The results in both cell lines showed that overexpressed IKK $\beta$  is sufficient to phosphorylate GST-I- $\kappa$ B $\alpha$ . While coexpressed TRAF1 showed no major effect on IKK $\beta$ -mediated GST-I- $\kappa$ B $\alpha$  phosphorylation, TRAF1-TD significantly reduced IKK $\beta$  activity, even after an additional stimulation with TNF or PMA (Fig. 5C). In all experiments TRAF1-TD coexpression resulted in a slightly reduced overall transfection efficiency. However, this effect is comparably minor and not sufficient to account for the observed reduction in IKK $\beta$  activity as is evident from the ratio of immunoprecipitated VSV-IKK $\beta$  and associated kinase activity.

**RIP, TRAF1, and the Caspase-generated Cleavage Product of TRAF1 Bind to the IKK Complex**—The results described above prompted us to test whether TRAF1 and/or TRAF1-(164–416)



**FIG. 5. The caspase-generated TRAF1 cleavage product inhibits NF- $\kappa$ B induction by signaling proteins acting upstream of p65.** *A*, HEK293 cells were cultured in 96-well plates and transfected with NF- $\kappa$ B and  $\beta$ -galactosidase reporter constructs, as described in the legend to Fig. 1, along with 0.03  $\mu$ g of expression vector of the indicated proteins and a 4-fold excess of either empty vector (*white bars*), or expression vectors for TRAF1 (*black bars*), and TRAF1-TD (*gray bars*). Reporter gene assays were carried out 18 h post-transfection. Relative values of NF- $\kappa$ B activity are indicated. *B*, HEK293 cells ( $5 \times 10^6$ ) were electroporated with a mixture of VSV-tagged IKK2 (1  $\mu$ g) and 9  $\mu$ g of either empty vector or expression vectors for TRAF1 and TRAF1-TD. Cells were seeded in 100-mm cell culture Petri dishes and cultivated for 18 h. Anti-VSV immunoprecipitates were analyzed by Western blotting with an antibody specific for IKK $\beta$  or were analyzed in immunocomplex kinase assays for IKK activity. *C*, Jurkat cells ( $1 \times 10^7$ ) were electroporated with a mixture of VSV-tagged IKK2 (10  $\mu$ g) and 30  $\mu$ g of either empty vector or expression vectors for TRAF1 and TRAF1-TD. Immediately after electroporation cells were split in 100-mm cell culture Petri dishes and cultivated overnight. The next day, cells were challenged with TNF (100 ng/ml) or a mixture of PMA (100 ng/ml) and ionomycin (2  $\mu$ g/ml) for 10 min or remained untreated. Again anti-VSV immunoprecipitates were analyzed by Western blotting with an antibody specific for IKK $\beta$  or were analyzed in immunocomplex kinase assays for IKK activity.

are associated with the IKK complex. In immunoprecipitates obtained with the anti-IKK $\alpha$  mAb B78-1, IKK $\beta$ , and IKK $\gamma$  specifically co-immunoprecipitated with IKK $\alpha$ , but not in controls using an isotype-matched mAb (data not shown). This indicated that B78-1 facilitates the immunoprecipitation of the intact IKK complex. Lysates of various cell lines were immunoprecipitated with an isotype-matched control antibody or anti-IKK $\alpha$  mAb, and the immunoprecipitates were analyzed with an anti-TRAF1 polyclonal antiserum by immunoblotting. Endogenous TRAF1 could be detected in the IKK complex of DII/23-7-, HeLa-, and SV80 cells using this approach (Fig. 6A). In IKK $\alpha$ -immunoprecipitates of apoptotic TRAF1-GFP transfectants, we found further co-immunoprecipitation of the caspase-derived carboxyl-terminal fragment of TRAF1-GFP (Fig. 6B), suggesting that the TRAF domain of TRAF1 is important for the association of TRAF1 with the IKK complex. Next we investigated TRAF1 association with the IKK complex in untreated DII/23-7 cells and cells treated for 7 and 60 min with TNF. We found no evidence for inducible changes in the association between TRAF1 and the IKK complex (Fig. 6C). For RIP, the IKK complex and the TNF-R1 signaling complex a transient interaction after TNF stimulation has been shown (26, 27). We therefore analyzed RIP-IKK complex association, too. In agreement with the cited reports, we found a transient interaction of RIP and the IKK complex, 7 min after TNF treatment (Fig. 6C).

*Association between the Caspase-derived TRAF1 Cleavage Product and the IKK Complex Involves the Amino-terminal Part of the TRAF Domain*—We and others (24, 28, 29) have

recently described that overexpression of TRADD leads to formation of distinct filaments, which can be used to identify proteins that interact with TRADD in living cells (24). Notably, the death domain of TRADD is completely sufficient for filament formation (24), whereas the amino-terminal region that facilitates associations with TRAF1 and TRAF2 (30) is dispensable. The biological significance of these filaments is not known. However, as ligand-induced activation of TNF-R1 leads to the formation of signaling competent receptor trimers and eventually secondary clustering of activated receptor complexes, it is possible that the TNF-R1-associated TRADD molecules might form comparable oligomerized structures. Such putative microfilaments may be partially equivalent to elongated filaments observed upon transient overexpression. This hypothesis is consistent with the finding that overexpressed TRADD exerts signaling capacities similar to activated TNF-R1 (30). In addition, proteins that interact endogenously with TRADD, such as TRAF1, TRAF2, RIP, and FADD are strongly recruited into TRADD filaments (data not shown). Moreover, these TRADD-interacting proteins can secondarily recruit additional molecules indirectly into TRADD filaments (24). This observation opened the possibility to use filament recruitment of GFP fusion proteins as a protein-protein interaction assay in living cells, not only for TRADD, but also for TRADD-bound molecules or proteins, which have been artificially targeted into filaments (filament interaction trap (FIT) assay).

We have employed the FIT assay to analyze the association between TRAF1 and the IKK complex further using a variety of

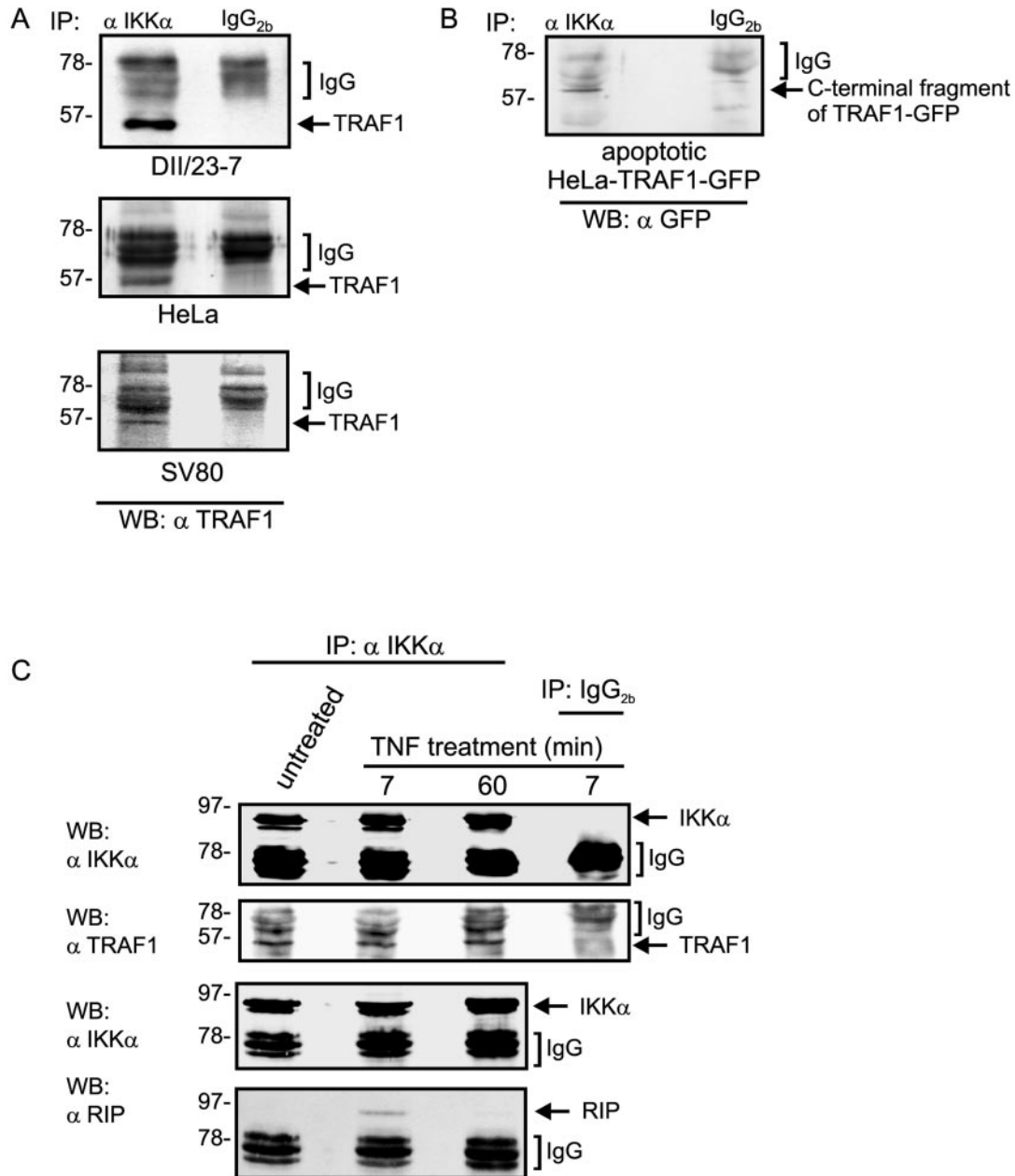


**FIG. 6. Interaction of TRAF1 with the IKK complex.** *A*, extracts of the indicated cells (DII/23-7:  $3 \times 10^8$ ; HeLa and SV80:  $1 \times 10^8$ ) were immunoprecipitated with IKK $\alpha$ -specific antibodies or an isotype-matched control antibody. Upon separation of the immunoprecipitate on a 12% SDS-PAGE co-immunoprecipitated endogenous TRAF1 was detected by immunoblotting with TRAF1-specific antibodies. Molecular Weight markers are shown on the left. *B*, interaction of TRAF1-GFP with the IKK complex. HeLa-TRAF1-GFP cells ( $1 \times 10^7$ ) were treated with TNF (100 ng/ml) and CHX (2.5  $\mu$ g/ml) for 6 h to induce apoptosis. Extracts of these cells were immunoprecipitated with IKK $\alpha$  antibodies or an isotype-matched control antibody and analyzed for co-immunoprecipitated GFP-tagged proteins by immunoblotting with a GFP-specific mAb. *C*, RIP interacts transiently with the IKK complex whereas TRAF1 is constitutively associated with this complex. DII/23-7 cells ( $3 \times 10^8$ ) were stimulated for the indicated times with TNF (50 ng/ml) and extracts derived of these cells were immunoprecipitated with IKK $\alpha$  antibodies. Co-immunoprecipitated endogenous molecules were detected with TRAF1- and RIP-specific antibodies. The precipitation of same amounts of the IKK complex was verified by immunoblotting with IKK $\alpha$  antibodies.

GFP/YFP-tagged proteins (Fig. 7A). The distribution of IKK $\alpha$ -YFP was not affected in cells, when TRADD was co-expressed. However, IKK $\alpha$ -YFP was detectable in filaments in triple transfections that included TRADD, IKK $\alpha$ -YFP, and either TRAF1 or TRAF1-TD, but not TRAF3 or TRAF3-TD expression constructs (Fig. 7B). Moreover, both TRAF1 and TRAF1-TD were also capable to facilitate recruitment of IKK $\beta$ -YFP and IKK $\gamma$ -GFP, but not GFP or a GFP fusion protein of the TRAF1-zinc finger domain (Fig. 7C and data not shown). Together, these data show that TRAF1 interacts with the IKK complex in a way that does not interfere with TRADD-TRAF1 interaction.

To investigate the association between the IKK complex and TRAF1-TD further, we generated a construct which encodes IKK $\gamma$  fused amino-terminal to the death domain of TRADD (IKK $\gamma$ -TRADD-(169-312) or IKK $\gamma$ -DD) (Fig. 7A). Similar to the DD of TRADD, this chimeric protein forms filaments, which strongly recruited co-expressed IKK $\alpha$ -YFP, IKK $\beta$ -YFP, and IKK $\gamma$ -GFP (Fig. 7D). Notably in a small fraction of cells (10-20%) that express high levels of IKK $\gamma$ -GFP, this fusion protein alone forms small granular aggregates. However, these structures are easily distinguishable from IKK $\gamma$ -DD filaments (Fig. 7E) and did not interfere with FIT analysis. Moreover, when

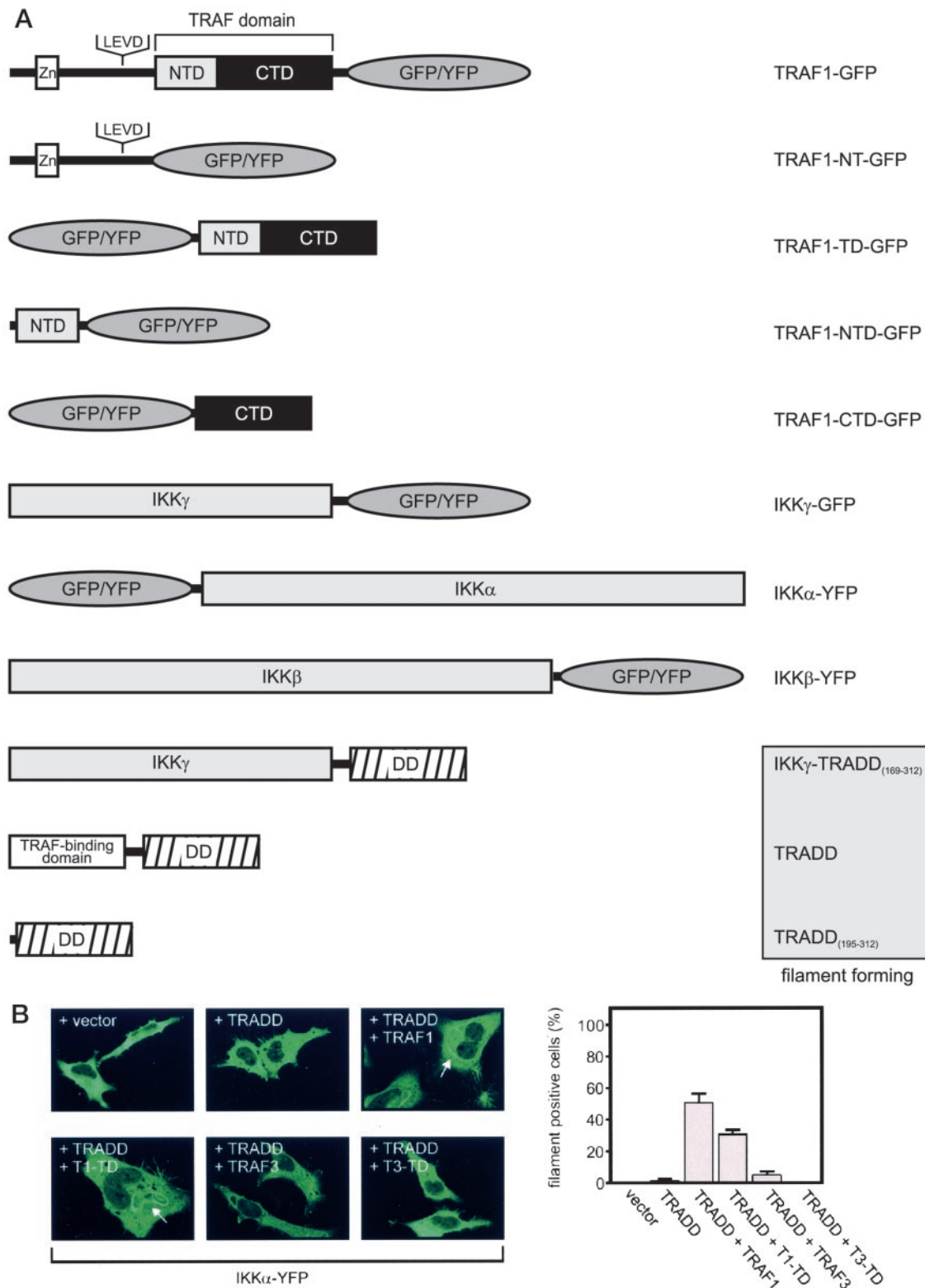


**FIG. 7. Analysis of the interaction of the IKK complex and TRAF1 and TRAF1-TD.** *A*, schema of constructs used for analysis of interaction of TRAF1 and TRAF1-TD with TRADD and the IKK complex. *B–F*, HeLa cells were grown on glass slides overnight and were subsequently transfected with a mixture of expression plasmids encoding the indicated proteins. To inhibit apoptosis induced by the death domain of TRADD cells were treated with z-VAD-fmk (20  $\mu$ M) immediately after transfection. Next day, transfected cells were analyzed by confocal microscopy. Recruitment of GFP fusion proteins into TRADD, TRADD-(195–312) or IKK $\gamma$ -TRADD-(165–312) filaments (white arrows) was quantified by calculating the percentage of transfected cells showing fluorescent filaments (bar diagram). Representative cells were selected for photography. *E*, up to 20% of cells transfected with IKK $\gamma$ -GFP (left panel) and less than 5% of cells co-transfected with IKK $\gamma$ -DD and IKK $\gamma$ -GFP (right panel) showed the indicated granular structures.

IKK $\gamma$ -GFP is co-transfected with IKK $\gamma$ -DD, the percentage of cells displaying IKK $\gamma$ -GFP granules decreased to below 5% (Fig. 7E). Similarly, a very small fraction of cells expressing

high levels of IKK $\beta$ -YFP displayed spike like structures (below 5%). Again these structures were clearly distinguishable from IKK $\gamma$ -DD filaments (data not shown). There was no recruit-

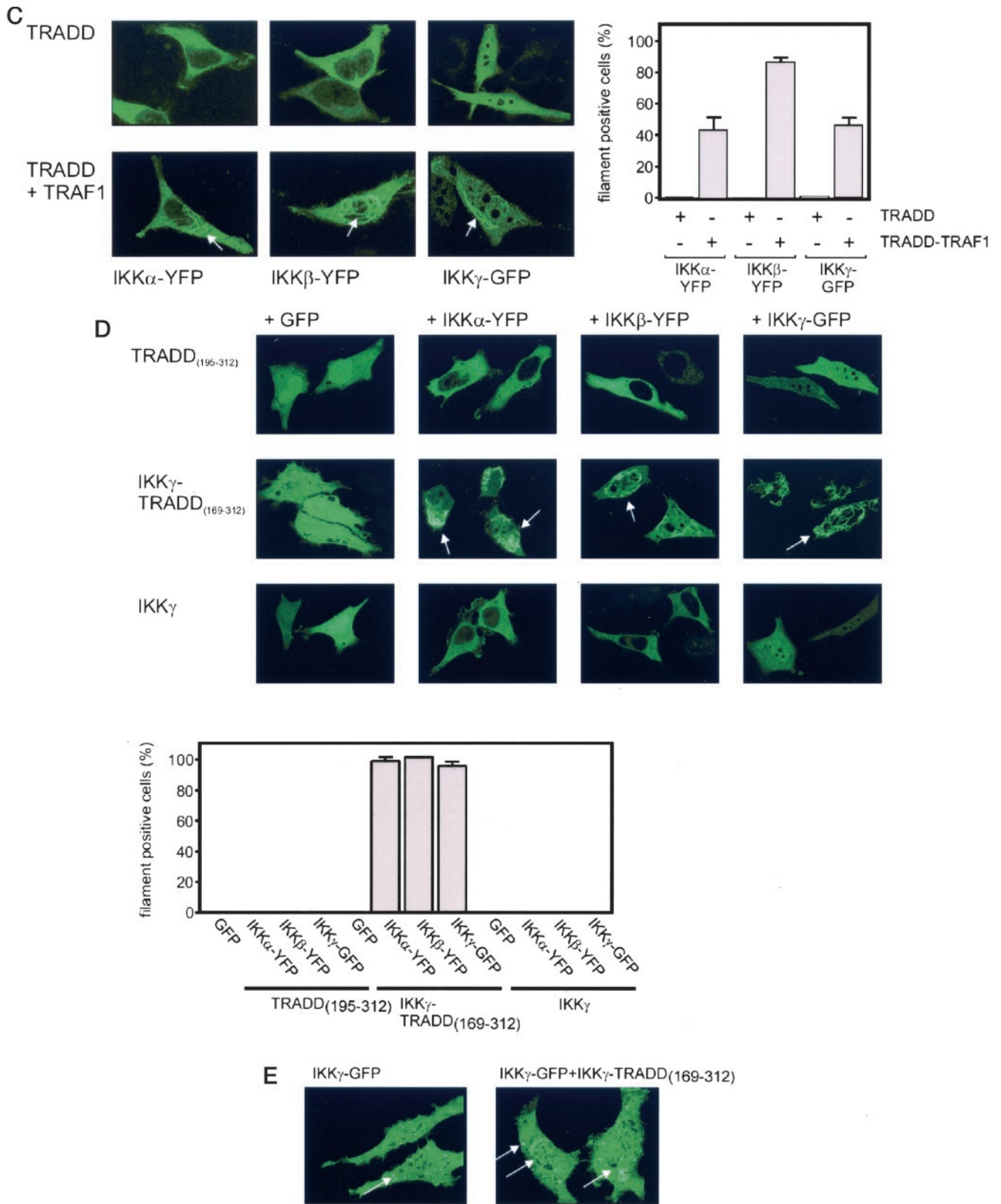


FIG. 7—continued

ment of IKK $\alpha$ -YFP, IKK $\beta$ -YFP, or IKK $\gamma$ -GFP to filaments, formed by the DD of TRADD (TRADD-(195–312)) alone (Fig. 7D). There were also no filamentous structures upon co-transfection of IKK $\gamma$  and the various GFP fusion proteins (Fig. 7D). These data demonstrate the usefulness of the IKK $\gamma$ -DD fusion protein to investigate IKK $\gamma$ -associated proteins by analysis of filament recruitment. TRAF1-GFP and TRAF1-TD-GFP, but

not a TRAF1 zinc-finger GFP fusion protein (TRAF1-NT-GFP), were recruited into IKK $\gamma$ -DD filaments (Fig. 7F). Again, none of these GFP/YFP fusion proteins were associated with TRADD-DD filaments or from filaments in concert with IKK $\gamma$  (Fig. 7F). Together, these observations confirm that the TRAF domain of TRAF1 mediates the interaction between TRAF1 and the IKK complex.

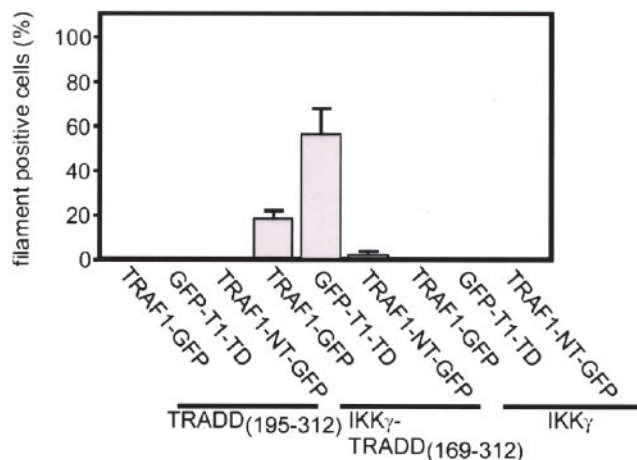
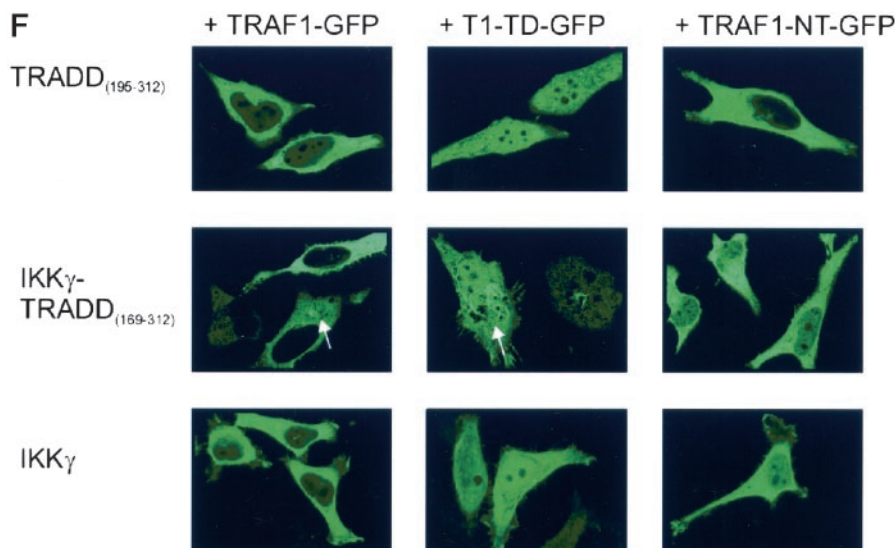
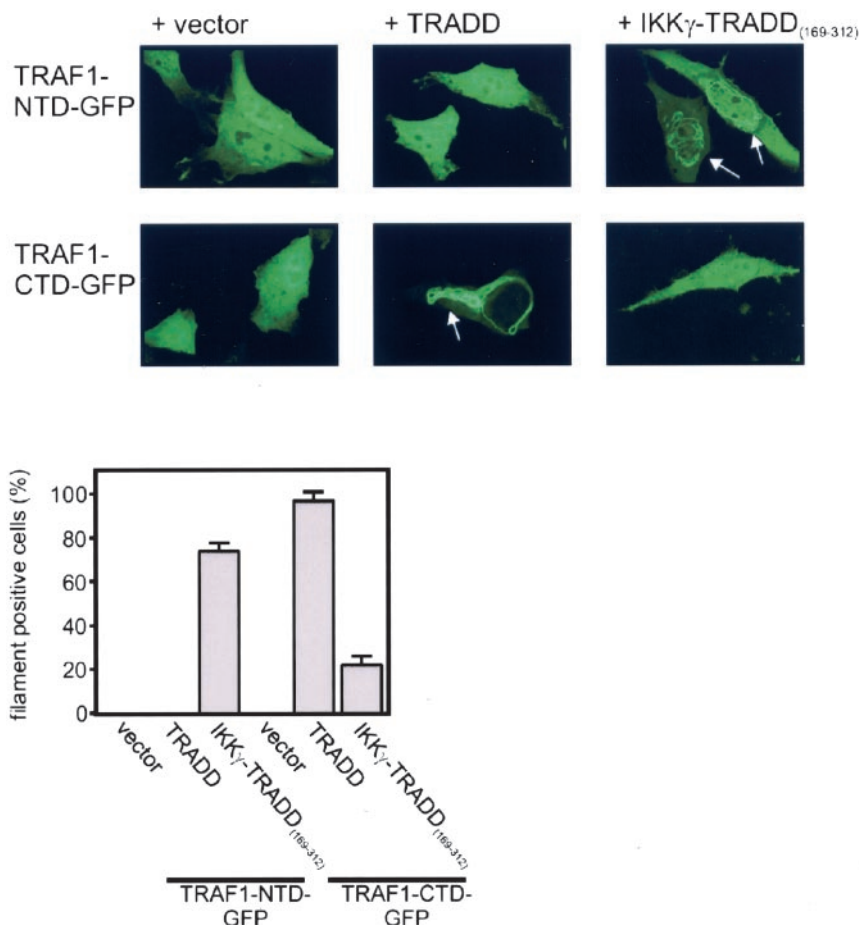


FIG. 7—continued

The TRAF domain of TRAF1 consists of a carboxyl-terminal subdomain (TRAF1-CTD), which is highly conserved among TRAF proteins and a less conserved amino-terminal region, the N-TRAF domain (TRAF1-NTD) (8). We have investigated the capacity of both subdomains to associate with the IKK complex or the amino-terminal TRAF-binding domain of TRADD by analyzing the recruitment of the GFP-tagged isolated subdomains into both IKK- $\gamma$ -DD and native TRADD filaments. The TRAF1-NTD-GFP fusion protein did not associate with full-length TRADD or the TRADD death domain, but it was strongly recruited into the IKK $\gamma$ -DD filaments (Fig. 8). In contrast, TRAF1-CTD-GFP associated with full-length TRADD, suggesting that this domain facilitates TRADD dependent interaction between TRAF1 and the TNF-R1 signaling complex. Notably, an interaction of TRAF1-CTD-GFP and IKK $\gamma$ -DD filaments was only barely detectable, with respect to both the portion of positive cells that showed filaments and the estimated intensity of filament recruitment (Fig. 8). These data suggest a primary role of the TRAF1-NTD in the interaction of both TRAF1 and its caspase-derived cleavage product with the IKK complex. We have tested whether TRAF1 can interact with a single component of the IKK complex using the two-hybrid system. In this assay TRAF1, but not TRAF3 was associated with IKK $\beta$ , as indicated by intensive blue staining of

yeast colonies, transformed with pGAD-TRAF1 and pAS2-IKK $\beta$ . In contrast, no association of neither TRAF1 nor TRAF3, was found with IKK $\alpha$  or IKK $\gamma$  (Table I). This observation suggests that TRAF1 interacts with the IKK complex via IKK $\beta$ . However, an additional role of HSP90 and its co-chaperone cdc37, which have been recently identified as part of the IKK-complex (31), cannot be ruled out. Further, we cannot exclude the possibility that IKK $\alpha$  or IKK $\gamma$  contribute to the association between the IKK complex and TRAF1/TRAF1-TD. A pivotal role of IKK $\beta$  for this interaction is also supported by FIT analysis, because the TRAF1-dependent recruitment of IKK $\beta$  to TRADD is significantly stronger than recruitment of IKK $\alpha$  and IKK $\gamma$  (Fig. 7C).

**Kinetic Analysis of the Interaction of the IKK Complex with TRAF1 and TRAF1-TD**—It is interesting to note that TRAF1-TD-GFP was much better recruited to IKK- $\gamma$ -DD filaments than TRAF1-GFP, although the expression levels of TRAF1-GFP were regularly higher than the expression of TRAF1-TD-GFP (data not shown). A possible explanation for this observation is that TRAF1-TD-GFP binds more strongly to the IKK complex than TRAF1-GFP. To investigate this further we performed FLIP and FRAP experiments with the TRAF1-GFP and TRAF1-TD-GFP occupied IKK $\gamma$ -DD filaments at 37 °C (Fig. 9). Using FLIP, we found that both molecules slowly dissociate



**FIG. 8. TRAF1 utilize distinct domains for interaction with TRADD and the IKK complex.** HeLa cells were grown on glass slides over night. To analyze interaction of the C-TRAF and N-TRAF domain of TRAF1 with TRADD and the IKK complex, cells were transfected with a mixture of expression plasmids encoding the indicated proteins in the presence of z-VAD-fmk (20  $\mu$ M). Next day, transfected cells were analyzed by confocal microscopy. Recruitment of GFP fusion proteins of the N-TRAF (TRAF1-NTD-GFP) and C-TRAF (TRAF1-CTD-GFP) domain of TRAF1 into TRADD and IKK $\gamma$ -TRADD-(165–312) filaments (white arrows) was quantified by calculating the percentage of transfected cells showing fluorescent filaments (bar diagram). Representative cells were selected for photography.

from the IKK $\gamma$ -DD filaments with an almost identical  $T_{1/2}$  of  $11.1 \pm 0.3$  (TRAF1-GFP) and  $11.3 \pm 0.3$  (TRAF1-TD-GFP) minutes. To characterize the association kinetics of both molecules we bleached TRAF1-GFP and TRAF1-TD-GFP occupied IKK $\gamma$ -DD filaments for 4 min and measured fluorescence recovery for an additional 10 min. As the association process is dependent on the concentration of the free molecules, we used for these experiments cells that showed comparable expression ( $\pm 20\%$  identical relative fluorescence units) of the GFP-tagged proteins. The 4-min bleaching pulse was restricted to the area occupied by the filament of interest and reduced the fluorescence intensity of TRAF1-GFP filaments in average from 141 to 63 relative units and the fluorescence intensity of TRAF1-TD-GFP from 135 to 60. The fluorescence intensity of the free unbound and therefore rapidly diffusing GFP fusion proteins was measured outside the bleach region and dropped down from 56 (TRAF1-GFP) and 43 relative fluorescence units to 50 and 39 units. This indicates that about 10% of the total cellular GFP-fusion proteins pool had been bleached. FRAP analysis of data corrected for this overall bleaching effect revealed that TRAF1-TD associates significantly faster than TRAF1-GFP to the bleached IKK $\gamma$ -DD filaments suggesting that the affinity of TRAF1-TD for the IKK complex is higher than the affinity of full-length TRAF1 (Fig. 9).

#### DISCUSSION

The functions of TRAF1 are still not completely understood. It was suggested that this molecule inhibits apoptosis, possibly via recruitment of anti-apoptotic factors, such as cIAP1 and cIAP2, into death receptor signaling complexes (11). The effects of TRAF1 on NF- $\kappa$ B activation are less clear. *In vivo* data suggest that TRAF1 selectively inhibits TNF-R2-induced

**TABLE I**  
Yeast two hybrid analysis of TRAF1 interactions with components of the IKK complex

Yeast strain Y187 were transformed with the listed plasmids. Yeast colonies were analyzed by  $\beta$ -galactosidase staining. Positive staining (+) or absence of staining (-) is indicated.

	pGBKT7-IKK $\alpha$	pAS2-IKK $\beta$	pBRIDGE-IKK $\gamma$
pGAD-TRAF1	-	+++	-
pGAD-TRAF3	-	-	-
pGAD	-	-	-

NF- $\kappa$ B activation in activated T-cells, but not CD40-induced NF- $\kappa$ B activation in B-lymphocytes (13). Moreover, a recent study with CD40L-matured bone marrow-derived dendritic cells showed reduced CD40-mediated NF- $\kappa$ B upon restimulation (17). Importantly, expression of TRAF2 was strongly reduced compared with CD40L-matured bone marrow-derived dendritic cells derived from wt mice (17). It is therefore possible that the observed reduction of CD40-mediated NF- $\kappa$ B activation is a consequence of the limited availability of TRAF2 and not an outcome of a direct NF- $\kappa$ B stimulatory action of TRAF1. In transient transfection experiments, both inhibitory and neutral to enhancing effects of TRAF1 have been reported on the activation of NF- $\kappa$ B (14–16). Remarkably, the TRAF1 gene is transcriptionally up-regulated by the NF- $\kappa$ B pathway (11, 15). As TRAF1 and the NF- $\kappa$ B pathway shows anti-apoptotic capabilities in most circumstances (12, 32), this argues against a common NF- $\kappa$ B-inhibitory role of TRAF1.

Consistent with our previous study, we found that TRAF1 inhibited CD40 mediated NF- $\kappa$ B activation in HEK293 cells

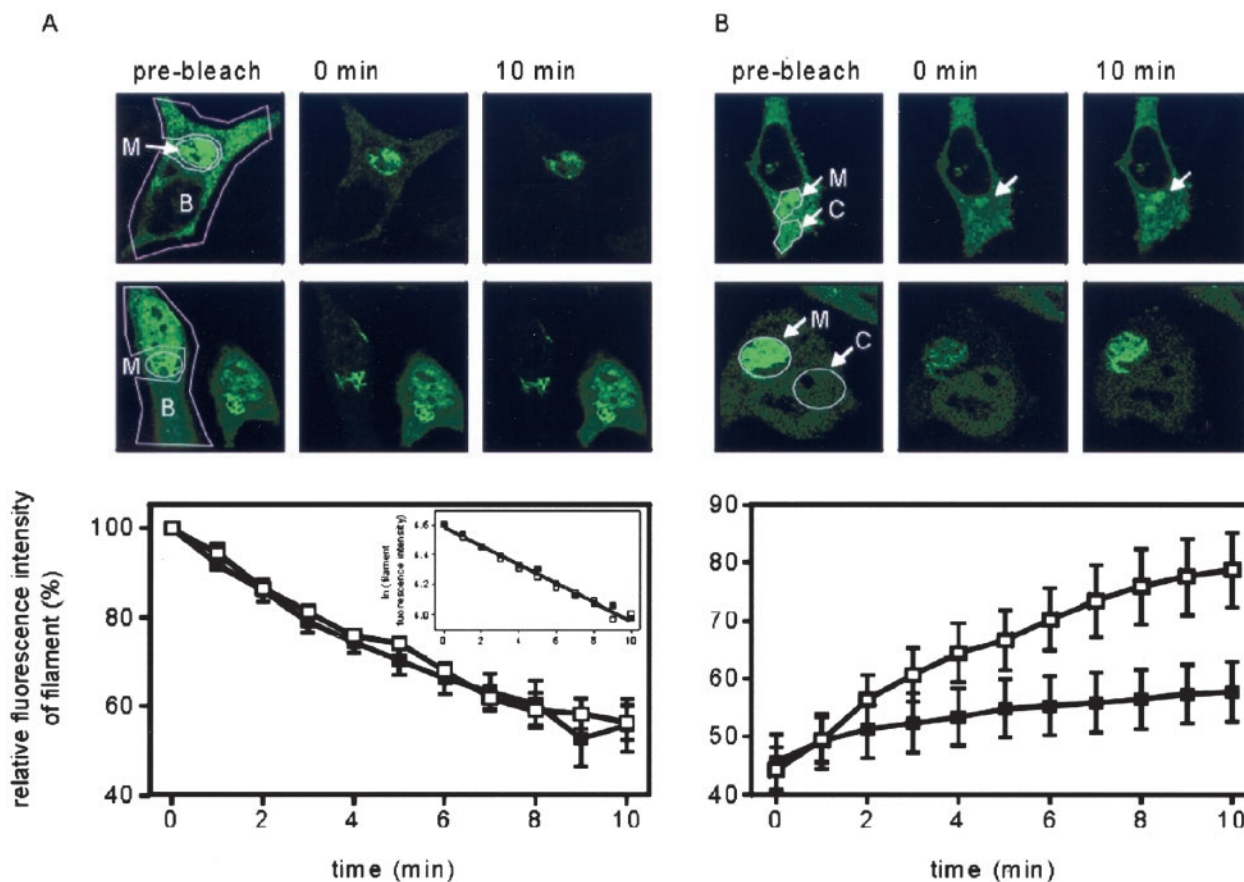


**FIG. 9. TRAF1 and TRAF1-D dissociate similarly from IKK $\gamma$ -TRADD-(165–312) filaments but exert different associations kinetics.** A, seven cells showing typical IKK $\gamma$ -DD filaments occupied with TRAF1-GFP (*upper microscopic panel; filled squares in diagram*) or TRAF1-TD-GFP (*lower microscopic panel, open squares in diagram*) was selected. A bleaching area covering the majority of the cell except the filament was defined (*B in microscopic panels*) and was initially bleached for 6 min to bleach the majority of the free highly diffusible GFP fusion proteins. Subsequently, dissociation of filament-associated GFP fusion proteins was monitored repetitive bleaching cycles of 1 min duration. Between each cycle an image was taken to determine the relative fluorescence intensities of the respective filament (*area M*). Measurements obtained for each filament were normalized against the relative filament fluorescence intensity obtained after the initial 6-min bleach. This time point of each experiment was defined as  $t = 0$  min. Averaged normalized relative fluorescence intensities were shown. To calculate the time ( $T_{1/2}$ ) when 50% of the bound GFP fusion proteins were released from the filaments, the dissociation curves were linearized by plotting the natural logarithm of the relative fluorescence intensities over time (*inset*).  $T_{1/2}$  values were calculated according to the equation  $T_{1/2} = \ln(2) / (\text{slope of regression})$  and were  $11.1 \pm 0.3$  min for TRAF1-GFP and  $11.3 \pm 0.3$  min for TRAF1-TD-GFP. B, to allow a fair comparison of the association behavior of TRAF1-GFP (*upper microscopic panel; filled squares in diagram*) and TRAF1-TD-GFP (*lower microscopic panel, open squares in diagram*) to IKK $\gamma$ -TRADD-(165–312) filaments cells with comparable expression of both GFP fusion proteins were selected. FRAP analysis was performed after a 4 min bleach pulse with high laser intensity on an area covering the filament (*B*). The bleach pulse resulted in reduction of filament fluorescence of about 55% for both GFP proteins and in a 10% reduction of the overall fluorescence of the free GFP proteins. Fluorescence intensity of filaments were determined every minute and normalized against the fluorescence intensity of the filament measured the 4-min bleach (already corrected for the overall bleach effect determined using the area C). Averaged normalized fluorescence intensities of filaments of different 8 cells were finally plotted against recovery time.

(Fig. 1). However, TRAF1 had no inhibitory effect when NF- $\kappa$ B was activated by TNF, IL-1, or overexpression of various components of the NF- $\kappa$ B signaling pathway including several members of the TNF receptor family (Figs. 1, 4, and 5). Since TRAF1 does not bind (33, 34) or only poorly binds (35) to CD40, the highly selective inhibition of NF- $\kappa$ B by this receptor must depend on interacting proteins or on inhibition of interaction of CD40 with TRAF2 which is critically involved in CD40-mediated NF- $\kappa$ B activation (36). Notably TRAF1 forms heteromers with TRAF2 and was suggested to modulate the signaling properties of this molecule (8). Consistent with this hypothesis, further analysis by confocal microscopy revealed that overexpression of TRAF1 specifically reduces the recruitment of TRAF2-GFP to clusters of activated CD40, but not to CD30, TNF-R2, or LT $\beta$ R (Fig. 2). Moreover, the caspase-generated TRAF1 fragment did also selectively modulate the TRAF2-GFP-CD40 interaction (Fig. 2). These findings suggest that TRAF2 heteromers containing TRAF1 or TRAF1-TD are less

efficiently recruited to activated CD40 than TRAF2 homomers. Such similar effects of TRAF1 and TRAF1-TD in respect to CD40-TRAF2 interaction are not unexpected as both oligomerization, as well as receptor interaction of TRAF proteins are dependent on the TRAF domain of these molecules (1–3). Importantly, full-length TRAF1 and TRAF1-TD differ significantly in their NF- $\kappa$ B inhibitory effects (Figs. 1 and 5) as only TRAF1-TD acts as a general inhibitor of NF- $\kappa$ B. As TRAF1-TD had no effect on TRAF2 recruitment to CD30 or TNF-R2, this general inhibitory effect cannot be related to differential regulation of TRAF receptor interaction. Taken together, our data suggest that full-length TRAF1 has no general effect on NF- $\kappa$ B signaling during the first few hours after this pathway has been activated but we cannot rule out that it could have an effect when long lasting or permanent NF- $\kappa$ B activation occurs. Nevertheless, TRAF1 can selectively regulate NF- $\kappa$ B activation at least one member of the TNF receptor family namely CD40. The effect of

full-length TRAF1 in a given cell type is possibly considerably dependent on the cell type specific expression pattern of interacting proteins that have been described for TRAF1 and/or other TRAF proteins (1–3). This might also explain why we did not observe an effect of TRAF1 on TNF-R2-induced NF- $\kappa$ B activation (Fig. 1) and TNF-R2-TRAF2 colocalization (Fig. 2) although TNF-R2-mediated NF- $\kappa$ B activation is enhanced in activated T-cells of TRAF1 knock-out mice (13). One should also take into consideration the possibility that TNF-R2-mediated NF- $\kappa$ B activation in T-cells is counteracted by TRAF1-TD as early after T-cell activation proliferation is dependent on the non-apoptotic activation of caspases (37–39). Thus, one cannot decide whether the reported increase of TNF-R2-mediated NF- $\kappa$ B activation in TRAF1<sup>-/-</sup> T-cells (13) is due to the absence of the NF- $\kappa$ B inhibitory TRAF1 fragment or due to the absence of full-length TRAF1.

TRAF1 was demonstrated to inhibit apoptosis (11, 12), but it is also a substrate of caspase-8 and the respective carboxyl-terminal fragment that is generated during apoptosis was previously shown to inhibit TNF mediated NF- $\kappa$ B activation (18, 19). Our functional analysis of this TRAF1 fragment discussed above revealed a remarkable difference to full-length TRAF1. TRAF1-TD, but not full-length TRAF1, inhibited NF- $\kappa$ B activation triggered by various NF- $\kappa$ B-inducing receptors (Fig. 1) and proteins, including RIP, TRADD, IKK $\beta$  (Fig. 5), but not p65. With respect to its broad and strong NF- $\kappa$ B inhibitory effect, TRAF1-TD is also functionally distinct from the corresponding TRAF domain-containing fragment being released from TRAF3 during apoptosis by caspase-mediated cleavage (Ref. 25 and Fig. 3) as the latter has no effect on NF- $\kappa$ B signaling (Fig. 4). Together these data indicate that TRAF1 is a unique TRAF protein that can be converted from a selective modulator of NF- $\kappa$ B activation into a generally acting inhibitor of the NF- $\kappa$ B pathway by caspase-mediated cleavage. The reporter gene data shown in Fig. 5A suggest that TRAF1-TD targets the NF- $\kappa$ B pathway downstream or at the level of the IKK complex. In accordance with this hypothesis, we found that TRAF1-TD but not full-length TRAF1, inhibits the enzymatic activity of the IKK complex (Fig. 5), the central component of the NF- $\kappa$ B signaling pathway, where signaling by a wide variety of NF- $\kappa$ B inducers converge (40, 41). In further accordance with the idea that the IKK complex is targeted by TRAF1 and TRAF1-TD, we found that both molecules associate with the endogenous IKK complex.

To characterize the interaction of the IKK complex and TRAF1 and TRAF1-TD, we analyzed the recruitment of GFP-tagged TRAF1 deletion mutants to an IKK $\gamma$ -DD fusion protein, which forms filaments by oligomerization via its death domain part. These experiments (Figs. 7 and 8) revealed that the N-TRAF subdomain of TRAF1 (8) is sufficient to allow interaction with the IKK complex. In contrast, the carboxyl-terminal C-TRAF domain of TRAF1 (8) was only weakly recruited to IKK $\gamma$ -DD filaments, but was sufficient for association with the amino-terminal TRAF-binding domain of TRADD and consequently the recruitment of TRAF1 into the TNF-R1 signaling complex. Yeast two-hybrid analysis supports the idea that IKK $\beta$  is the component of the IKK complex that is targeted by TRAF1. This is also consistent with FIT analyses, showing a significantly stronger TRAF1-dependent recruitment of IKK $\beta$ -YFP to TRADD filaments, as compared with IKK $\alpha$ -GFP or IKK $\gamma$ -YFP (Fig. 7C). It is interesting to note that two distinct subdomains of TRAF1-TD are utilized to interact with TRADD and the IKK complex, respectively, suggesting that TRAF1-TD inhibits NF- $\kappa$ B signaling also when this complex is recruited to TNF-R1. Although full-length TRAF1 and the cleavage product

TRAF1-TD associate with the IKK complex, only TRAF1-TD inhibits its kinase activity (Fig. 5B). The basis for these different effects is not yet clear. However, analysis of IKK $\gamma$ -DD filament-recruited TRAF1-GFP and TRAF1-TD-GFP allows some speculations. Recruitment of TRAF1-TD-GFP to IKK $\gamma$ -DD filaments is significantly more efficient than recruitment of TRAF1-GFP in terms of percentage of transfected cells showing recruitment and also in respect of recruitment efficiencies (Fig. 7C). This suggests that the affinity of TRAF1-TD to the IKK $\gamma$  part of IKK $\gamma$ -DD filaments is higher as compared with full-length TRAF1. FLIP experiments showed that both TRAF1-GFP and TRAF1-TD-GFP indistinguishably dissociate from IKK $\gamma$ -DD filaments with a T<sub>1/2</sub> of about 11 min (Fig. 9). However, FRAP experiments demonstrated that TRAF1-TD-GFP associates faster to IKK $\gamma$ -DD filaments than TRAF1-GFP (Fig. 9). Thus, the observed increased affinity of TRAF1-TD to IKK $\gamma$ , compared with TRAF1 appears to be caused mainly by an increased association rate. Based on these protein-protein interaction data, obtained in living cells, a possible explanation for the inhibitory effect of TRAF1-TD is that this apoptosis-related fragment interacts more strongly with a regulatory site of the IKK complex that channels the action of diverse upstream activators of the IKK complex and thereby prevents its activation.

## REFERENCES

1. Wajant, H., Henkler, F., and Scheurich, P. (2001) *Cell Signal.* **13**, 389–400
2. Bradley, J. R., and Pober, J. S. (2001) *Oncogene* **20**, 6482–6491
3. Chung, J. Y., Park, Y. C., Ye, H., and Wu, H. (2002) *J. Cell Sci.* **115**, 679–688
4. Shiels, H., Li, X., Schumacker, P. T., Maltepe, E., Padrid, P. A., Sperling, A., Thompson, C. B., and Lindsten, T. (2000) *Am. J. Pathol.* **157**, 679–688
5. Regnier, C. H., Masson, R., Kedinger, V., Textoris, J., Stoll, I., Chenard, M. P., Dierich, A., Tomasello, C., and Rio, M. C. (2002) *Proc. Natl. Acad. Sci. U. S. A.* **99**, 5585–5590
6. Masson, R., Regnier, C. H., Chenard, M. P., Wendling, C., Mattei, M. G., Tomasello, C., and Rio, M. C. (1998) *Mech. Dev.* **71**, 187–191
7. Krajewska, M., Krajewski, S., Zapata, J. M., Van Arsdale, T., Gascoyne, R. D., Berern, K., McFadden, D., Shabaik, A., Hugh, J., Reynolds, A., Cleveland, C. V., and Reed, J. C. (1998) *Am. J. Pathol.* **152**, 1549–1561
8. Rothe, M., Wong, S. C., Henzel, W. J., and Goeddel, D. V. (1994) *Cell* **78**, 681–692
9. Mosialos, G., Birkenbach, M., Yalamanchili, R., VanArsdale, T., Ware, C., and Kieff, E. (1995) *Cell* **80**, 389–399
10. Rothe, M., Pan, M. G., Henzel, W. J., Ayres, T. M., and Goeddel, D. V. (1995) *Cell* **83**, 1243–1252
11. Wang, C. Y., Mayo, M. W., Korneluk, R. G., Goeddel, D. V., and Baldwin, A. S., Jr. (1998) *Science* **281**, 1680–1683
12. Speiser, D. E., Lee, S. Y., Wong, B., Arron, J., Santana, A., Kong, Y. Y., Ohashi, P. S., and Choi, Y. (1997) *J. Exp. Med.* **185**, 1777–1783
13. Tsitsikov, E. N., Laouini, D., Dunn, I. F., Sannikova, T. Y., Davidson, L., Alt, F. W., and Geha, R. S. (2001) *Immunity* **15**, 647–657
14. Duckett, C. S., Gedrich, R. W., Gilfillan, M. C., and Thompson, C. B. (1997) *Mol. Cell. Biol.* **17**, 1535–1542
15. Schwenzler, R., Siemienski, K., Liptay, S., Schubert, G., Peters, N., Scheurich, P., Schmid, R. M., and Wajant, H. (1999) *J. Biol. Chem.* **274**, 19368–19374
16. Carpentier, I., and Beyaert, R. (1999) *FEBS Lett.* **460**, 246–250
17. Arron, J. R., Pewzner-Jung, Y., Walsh, M. C., Kobayashi, T., and Choi, Y. (2002) *J. Exp. Med.* **196**, 923–934
18. Irmiler, M., Steiner, V., Ruegg, C., Wajant, H., and Tschopp, J. (2000) *FEBS Lett.* **468**, 129–133
19. Leo, E., Deveraux, Q. L., Buchholtz, C., Welsh, K., Matsuzawa, S., Stennicke, H. R., Salvesen, G. S., and Reed, J. C. (2001) *J. Biol. Chem.* **276**, 8087–8093
20. Birbach, A., Gold, P., Binder, B. R., Hofer, E., de Martin, R., and Schmid, J. A. (2002) *J. Biol. Chem.* **277**, 10842–10851
21. Wajant, H., Johannes, F. J., Haas, E., Siemienski, K., Schwenzler, R., Schubert, G., Weiss, T., Grell, M., and Scheurich, P. (1998) *Curr. Biol.* **8**, 113–116
22. Lee, S. Y., Park, C. G., and Choi, Y. (1996) *J. Exp. Med.* **183**, 669–674
23. Gedrich, R. W., Gilfillan, M. C., Duckett, C. S., Van Dongen, J. L., and Thompson, C. B. (1996) *J. Biol. Chem.* **271**, 12852–12858
24. Fotin-Mlecsek, M., Henkler, F., Samel, D., Reichwein, M., Hausser, A., Parmryd, I., Scheurich, P., Schmid, J. A., and Wajant, H. (2002) *J. Cell Sci.* **115**, 2757–2770
25. Lee, Z. H., Lee, S. E., Kwack, K., Yeo, W., Lee, T. H., Bae, S. S., Suh, P. G., and Kim, H. H. (2001) *J. Leukoc. Biol.* **69**, 490–496
26. Zhang, S. Q., Kovalenko, A., Cantarella, G., and Wallach, D. (2000) *Immunity* **12**, 301–311
27. Devin, A., Cook, A., Lin, Y., Rodriguez, Y., Kelliher, M., and Liu, Z. (2000) *Immunity* **12**, 419–429
28. Inada, H., Izawa, I., Nishizawa, M., Fujita, E., Kiyono, T., Takahashi, T., Momoi, T., and Inagaki, M. (2001) *J. Cell Biol.* **155**, 415–426

29. Morgan, M., Thorburn, J., Pandolfi, P. P., and Thorburn, A. (2002) *J. Cell Biol.* **157**, 975–984
30. Hsu, H., Shu, H. B., Pan, M. G., and Goeddel, D. V. (1996) *Cell* **84**, 299–308
31. Chen, G., Cao, P., and Goeddel, D. V. (2002) *Mol. Cell* **9**, 401–410
32. Karin, M., and Lin, A. (2002) *Nat. Immunol.* **3**, 221–227
33. Leo, E., Welsh, K., Matsuzawa, S., Zapata, J. M., Kitada, S., Mitchell, R. S., Ely, K. R., and Reed, J. C. (1999) *J. Biol. Chem.* **274**, 22414–22422
34. Pullen, S. S., Labadia, M. E., Ingraham, R. H., McWhirter, S. M., Everdeen, D. S., Alber, T., Crute, J. J., and Kehry, M. R. (1999) *Biochemistry* **38**, 10168–10177
35. Pullen, S. S., Miller, H. G., Everdeen, D. S., Dang, T. T. A., Crute, J. J., and Kehry, M. R. (1998) *Biochemistry* **37**, 11836–11845
36. Nguyen, L. T., Duncan, G. S., Mirtsos, C., Ng, M., Speiser, D. E., Shahinian, A., Marino, M. W., Mak, T. W., Ohashi, P. S., and Yeh, W. C. (1999) *Immunity* **11**, 379–389
37. Kennedy, N. J., Kataoka, T., Tschopp, J., and Budd, R. C. (1999) *J. Exp. Med.* **190**, 1891–1896
38. Alam, A., Cohen, L. Y., Aouad, S., and Sekaly, R. P. (1999) *J. Exp. Med.* **190**, 1879–1890
39. Mack, A., and Hacker, G. (2002) *Eur. J. Immunol.* **32**, 1986–1992
40. Silverman, N., and Maniatis, T. (2001) *Genes Dev.* **15**, 2321–2342
41. Ghosh, S., and Karin, M. (2002) *Cell* **109**, 81–96